14 H, linoleyl aliphatic H's), 1.21 (d, 3 H, J = 6.3 Hz, Thr C_4-H_3), 1.18 (d, 3 H, J = 6.4 Hz, Thr C_4-H_3), 1.04 (d, 3 H, J = 6.9 Hz, Hmp C_3-CH_3), 0.90 (t, 3 H, J = 6.9 Hz, linoleyl CH_3); $[\alpha]_D$ -43° (c 0.82, MeOH) (lit.[1a] $[\alpha]_D$ -45.5° (c 0.81, MeOH)); MS (FAB, m-nitrobenzyl alcohol) m/z 1012 (M + 1).

Tetrahydroechinocandin D. This reaction was carried out according to the procedure of v. Wartburg and co-workers.[1a] A solution of 25.4 mg of echinocandin D in 3 mL of ethanol was stirred over 10% Pd-C under an atmospliere of hydrogen for 3 h. It was then filtered through Celite and concentrated to give a glass: R_f 0.34 (20% methanol/methylene chloride); HPLC (Vydak, 10% water/methanol, 1.5 mL/min, 280-nm detection) t_r 5.20 min; IR (Nujol) 3700-2500 (br), 1690-1620 (br), 1537, 1518, 1350 (br), 1240 (br), 1077, 720 cm^{-1}; ^1H NMR (500 MHz, CD_3OD) δ 6.99 (d, 2 H, J = 8.4 Hz, aromatic H's), 6.68 (d, 2 H, J = 8.4 Hz, aromatic H's), 4.89 (overlapping d, 2 H, J = 3.9 Hz, Thr C_2-H, Thr C_2-H), 4.64 (dd, 1 H, J = 7.0, 11.4 Hz, Hyp C_2-H), 4.57 (br s, 1 H, Hyp C_4-H), 4.48-4.44 (m, 1 H, Thr C_3-H), 4.41 (br s, 1 H, Hht C_2-H), 4.40-4.36 (m, 2 H, Orn C_2-H, Hht C_3-H), 4.31 (d, J = 2.5 Hz, 1 H, Hmp C_2-H), 4.26-4.22 (m, 1 H, Thr C_2-H), 4.14 (dd, 1 H, J = 2.5, 4.4 Hz, Hmp C_3-H), 4.00 (dd, 1 H, J = 3.3, 11.0 Hz, Hyp C_5-H), 3.85 (dd, 1 H, J = 7.5, 9.2 Hz, Hmp C_5-H), 3.80 (d, 1 H, J = 11.0 Hz, Hyp C_5-H), 3.49-3.43 (m, 1 H, Orn C_5-H), 3.38 (t, 1 H, J = 9.2 Hz, Hmp C_5-H), 2.99-2.95 (m, 1 H, Orn C_5-H), 2.64 (dd, 1 H, J = 6.4, 13.7 Hz, Hht C_4-H), 2.55 (dd, 1 H, J = 7.8, 13.7 Hz, Hht C_4-H), 2.49-2.43 (m, 2 H, Hyp C_3-H, Hmp C_4-H), 2.23 (two overlapping dt, 2 H, J = 7.4, 15.0 Hz, $COCH_2$), 2.15-2.04 (m, 2 H, Orn C_3-H, Hyp C_3-H), 1.72-1.66 (m, 2 H, Orn C_4-H_2), 1.62-1.51 (m, 3 H, Orn C_3-H, $COCH_2CH_2$), 1.41-1.28 (m, 2 H, $COCH_2CH_2CH_2$), 1.28 (s, 26 H, stearoyl H's), 1.22 (d, 3 H, J = 6.3 Hz, Thr C_4-H_3), 1.18 (d, 3 H, J = 6.4 Hz, Thr C_4-H_3), 1.05 (d, 3 H, J = 6.8 Hz, Hmp C_3-CH_3), 0.89 (t, 3 H, J = 6.9 Hz, stearoyl CH_3); $[\alpha]_D$ -42° (c 0.59, MeOH) (natural: $[\alpha]_D$ -42° (c 0.59, MeOH)); MS (FAB, m-nitrobenzyl alcohol) m/z 1016 (M + 1).

Acknowledgment. We thank Dr. Y. Ohfune, Suntory Institute, for kindly providing a sample of echinocandin D, as well as spectroscopic data for **20**, **21**, **23**, echinocandin D, and tetrahydroechinocandin D. We also thank Dr. A. v. Wartburg, Sandoz AG, for providing a generous sample of tetrahydroechinocandin D. Support from the National Science Foundation (Predoctoral Fellowship (1982-1985) for A.E.W.) and the National Institutes of Health is gratefully acknowledged. The NIH BRS Shared Instrumentation Grant Program 1 S10 RR01748-01A1 is acknowledged for providing NMR facilities.

X-ray Absorption Spectroscopy of Metal-Histidine Coordination in Metalloproteins. Exact Simulation of the EXAFS of Tetrakis(imidazole)copper(II) Nitrate and Other Copper-Imidazole Complexes by the Use of a Multiple-Scattering Treatment

Richard W. Strange,[1a] Ninian J. Blackburn,[1a] P. F. Knowles,[1b] and S. Samar Hasnain*[1c]

Contribution from the Department of Chemistry, University of Manchester Institute of Science and Technology, Manchester, M60 1QD, United Kingdom, and S.E.R.C. Daresbury Laboratory, Warrington, Cheshire, WA4 4AD, United Kingdom. *Received January 26, 1987*

Abstract: Histidine coordination occurs in many metalloproteins, but analysis of the contributions to the EXAFS of the outer shells of atoms of the imidazole rings has, in the past, proved difficult. An exact method for simulating the raw experimental EXAFS over the complete energy range (k = 2-16 Å^{-1}) is reported and applied to the simulation of tetrakis(imidazole)copper(II) nitrate, tetrakis(imidazole)copper(II) perchlorate, and aquatris(imidazole)copper(II) sulfate. It is shown that strong multiple-scattering contributions are present in the EXAFS over an extended range above the absorption edge and these contributions are necessary to fix the third-shell atoms of the imidazole groups at their correct positions. Furthermore, by including multiple scattering in the EXAFS analysis, it is possible to extend the low-energy fitting range to include the XANES region of the spectrum below k = 3, the general shape of this part of the spectrum being well reproduced. In favorable circumstances, the multiple-scattering approach can provide the basis for determining the number of histidine ligands in a mixed-ligand complex and can clearly distinguish between two and four coordinated imidazole groups, although distinction between three and four histidines is probably unrealistic for a metalloprotein site of unknown structure.

In recent years, X-ray absorption spectroscopy has been used to probe the environment of transition metals at the active sites of metalloproteins and other biologically important molecules. By analyzing the high-energy (EXAFS) region of the X-ray spectrum, useful information concerning the distance, type, and number of atoms coordinated at the metal site has been obtained.[2-4] For metalloenzymes whose X-ray absorption spectrum is dominated by the presence of histidine ligands, this information has often been restricted to the first- and sometimes second-shell coordination spheres, extending ca. 3.2 Å from the absorbing atom. Atoms belonging to imidazole rings lying beyond this distance have proved more difficult to simulate. Methods employing parameterization of the amplitudes and phase-shift functions,[3-6]

(1) (a) Department of Chemistry, University of Manchester Institute of Science and Technology, UK. (b) Department of Biophysics, University of Leeds, UK. (c) S.E.R.C. Daresbury Laboratory, Warrington, Cheshire, UK.

(2) (a) *EXAFS and Near Edge Structure III, Proceedings of the International Conference, Stanford*; Hodgson, K. O., Hedman, B. O., Penner-Hahn, J. E., Eds.; Springer: Berlin, 1983; *Springer Proc. Phys.* **1983**, *1*. (b) Teo, B. K. In *EXAFS Spectroscopy: Techniques and Applications*; Teo, B. K., Joy, D. C., Eds.; Plenum: New York, 1981; pp 13-58. (c) Cramer, S. P.; Hodgson, K. O. *Prog. Inorg. Chem.* **1979**, *25*, 1-39. (d) Garner, C. D.; Helliwell, J. R. *Chem. Br.* **1986**, *22*, 835-840.

(3) Cramer, S. P.; Hodgson, K. O.; Stiefel, E. I.; Newton, W. E. *J. Am. Chem. Soc.* **1978**, *100*, 2748-2761.

(4) (a) Co, M. S.; Scott, R. A.; Hodgson, K. O. *J. Am. Chem. Soc.* **1981**, *103*, 986-988. (b) Co, M. S.; Hodgson, K. O. *J. Am. Chem. Soc.* **1981**, *103*, 3200-3201. (c) Co, M. S.; Hodgson, K. O.; Eccles, T. K.; Lontie, R. *J. Am. Chem. Soc.* **1981**, *103*, 984-986.

(5) (a) Brown, J. M.; Powers, L.; Kincaid, B.; Larrabee, J. A.; Spiro, T. G. *J. Am. Chem. Soc.* **1980**, *102*, 4210-4216. (b) Woolery, G. L.; Powers, L.; Winkler, M.; Solomon, E. I.; Spiro, T. G. *J. Am. Chem. Soc.* **1984**, *106*, 86-92. (c) Woolery, G. L.; Powers, L.; Winkler, M.; Solomon, E. I.; Lerch, K.; Spiro, T. G. *Biochim. Biophys. Acta* **1984**, *788*, 155-161. (d) Woolery, G. L.; Powers, L.; Peisach, J.; Spiro, T. G. *Biochemistry* **1984**, *23*, 3428-3434.

0002-7863/87/1509-7157$01.50/0

including imidazole group fitting routines,[4] have met with some success but have been unable to treat the differences in experimental EXAFS and Fourier transforms that result from differences in imidazole ring orientation.[6] On the other hand, ab initio simulations of unfiltered EXAFS data, using single-scattering theory, give satisfactory fits to the data only if the outer-shell atoms of the imidazole rings are placed ca. 0.3 Å shorter than the distance expected on the basis of the first-shell Cu–N bond length.[7] A similar foreshortening of outer-shell (pyrrole C3/C4) distances has been found in the analysis of heme systems.[8]

It is clear that the single-scattering EXAFS theory used in these studies is inadequate to describe the low-energy region of the unfiltered experimental spectrum, where longer range scattering interactions become most significant. Furthermore, the inability to interpret this region of the spectrum results in valuable structural information being discarded. For example, the subtle changes in amplitude of the first EXAFS beat that have been observed by Chance and co-workers in their studies on myoglobin, cytochrome-*c* peroxidase, and their derivatives with hydrogen peroxide[9] have suggested the existence of an empirical relationship between EXAFS beat amplitude and the spin-state/coordination number of the iron. Theoretical treatment of the low-energy region of the spectrum would provide a more reliable basis for the structural interpretation of such observations.

We[7] and others[6] have suggested that the anomalous results obtained for outer-shell atoms of histidine ligands may be due to multiple-scattering processes occurring within the imidazole rings, which are not taken into account in the single-scattering theory. The present study provides the first quantitative examination of this problem. Since multiple-scattering effects are dependent on the geometry of the ligands in the metal site, our study has initially been concerned with an analysis of these effects in crystallographically well-characterized compounds having copper as the absorbing atom, coordinated to three or four imidazole groups. These compounds therefore serve as models for the active sites of copper-containing enzymes known or believed to have histidine ligands coordinated to copper,[10] including Cu/Zn superoxide dismutase,[11] plasma amine oxidases,[12] and dopamine β-hydroxylase.[13] Our results clearly demonstrate that strong multiple-scattering contributions are present in the EXAFS over an extended energy range above the absorption edge and that these contributions must be included in the EXAFS analysis in order to simulate correctly the outer-shell atoms of the imidazole rings.

Materials and Methods

The model compounds used were tetrakis(imidazole)copper(II) nitrate,[14] tetrakis(imidazole)copper(II) perchlorate,[15] and aquatris(imidazole)copper(II) sulfate.[16] The complexes were synthesized by literature methods and recrystallized from ethanol–water mixtures. Samples were measured as powders. X-ray absorption measurements were performed at 77 K in the transmission mode, using beam line 7.1 at the Synchrotron Radiation Source (SRS), SERC Daresbury Laboratory. The SRS was operated at 2.0 GeV with maximum beam currents of 300 mA.

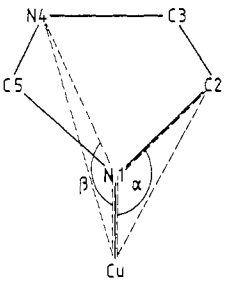

Figure 1. Representation of an imidazole ring showing the atom-labeling scheme. The important multiple-scattering pathways are shown as dashed lines and are the angles refined in the multiple-scattering calculations.

Analysis of the data was performed with a NAS 7000 series computer. EXAFS simulations were carried out by using the program EXCURVE,[17] which is based upon the spherical wave theory developed by Lee and Pendry.[18] Multiple-scattering calculations were carried out within EXCURVE by defining the geometry of the imidazole rings from the known crystallographic data and then submitting a background job using the program EXFIT (N. Binsted, unpublished).

After background subtraction the experimental EXAFS was transformed into k space, where $k^2 = 0.263\ (E - E_0)$, E is the energy of the X-ray beam, and E_0 is the energy threshold of the photoelectron wave. The EXAFS spectra were weighted by k^3 to compensate for the diminishing amplitude at high k values. Least-squares refinement of several parameters was made to obtain the best fit to the experimental data. Refinement in single-scattering calculations was limited to the distance parameters and E_0; the coordination numbers were fixed by their crystallographic values and the Debye–Waller terms were determined from a visual comparison of experiment and theory for both EXAFS and Fourier transform peaks. In multiple-scattering calculations the radial distances of the outer-shell atoms and E_0 were iterated, and the single-scattering EXAFS contribution was added as a constant at each step of the iteration. The revised parameters from the multiple-scattering calculations were then used to recalculate the single-scattering contribution, which was then added to the multiple-scattering EXAFS. This procedure was repeated until further refinement of the positions of the otuer-shell atoms resulted in only minor (<0.02 Å) changes in their values. The parameters defining the angular distribution of the second- and third-shell atoms of the imidazole rings (Figure 1) were also refined by iteration until self-consistency was achieved.

Atomic phase shifts were calculated by ab initio methods, as described previously[7b,8] using the program MUFPOT. In this program a complex electronic potential is constructed within the muffin-tin approximation using Clementi–Roetti wave functions.[19] Electron exchange and correlation effects are accounted for. The excited central atom is represented by the wave functions of a neutral ($Z + 1$) atom where the occupancy of the 1s orbital is reduced to one. The phase-shift calculations were accomplished by using tetrakis(imidazole)copper(II) nitrate as a model structure for the determination of muffin-tin radii, and the nitrogen phase shift was further refined by fitting a theoretical wave to the Fourier-filtered first shell of the tetrakis(imidazole)copper(II) complex. The refined and calculated phase shifts differ by <5% and give a difference in Cu–N distance of <0.02 Å.

Multiple-Scattering Theory

Multiple-scattering effects were first observed in the EXAFS of copper foil by Lee and Pendry,[18] where the fourth-shell scat-

(6) The amplitudes of the outer shells in the Fourier transforms of the Zn and Co K-edge EXAFS of carbonic anhydrase derivatives are dependent on pH and suggest changes in imidazole ring orientation among the derivatives studied. Yachandra, V.; Powers, L.; Spiro, T. G. *J. Am. Chem. Soc.* **1983**, *105*, 6596–6604.

(7) (a) Blackburn, N. J.; Hasnain, S. S.; Diakun, G. P.; Knowles, P. F.; Binsted, N.; Garner, C. D. *Biochem. J.* **1983**, *213*, 765–768. (b) Blackburn, N. J.; Hasnain, S. S.; Binsted, N.; Diakun, G. P.; Garner, C. D.; Knowles, P. F. *Biochem. J.* **1984**, *219*, 985–990.

(8) Perutz, M. F.; Hasnain, S. S.; Duke, P. J.; Sessler, J. L.; Hahn, J. E. *Nature (London)* **1982**, *295*, 535–538.

(9) (a) Chance, M.; Powers, L.; Poulos, T.; Chance, B. *Biochemistry* **1986**, *25*, 1266–1270. (b) Chance, M.; Powers, L.; Kumar, C.; Chance, B. *Biochemistry* **1986**, *25*, 1259–1265.

(10) (a) *Copper Proteins and Copper Enzymes*; Lontie, R., Ed.; CRC Press: Boca Raton, FL, 1984; Vol. 1–3. (b) *Biological and Inorganic Copper Chemistry* (Proceedings of the 2nd Conference on Copper Coordination Chemistry, Albany); Karlin, K. D., Zubieta, J., Eds.; Adenine: Guilderland, NY, 1986; Vol. 1, 2.

(11) (a) Tainer, J. A.; Getzoff, E. D.; Beem, K. M.; Richardson, J. S.; Richardson, D. C. *J. Mol. Biol.* **1982**, *160*, 181–217.

(12) (a) Knowles, P. F.; Yadav, K. D. S. In *Copper Proteins and Copper Enzymes*; Lontie, R., Ed.; CRC Press: Boca Raton, FL, 1984; Vol. 2, pp 103–129. (b) Baker, G. J.; Knowles, P. F.; Pandeya, K. B.; Rayner, B. J. *Biochem. J.* **1986**, *237*, 609–612. (c) Scott, R. A.; Dooley, D. M. *J. Am. Chem. Soc.* **1985**, *107*, 4348–4350.

(13) Hasnain, S. S.; Diakun, G. P.; Knowles, P. F.; Binsted, N.; Garner, C. D.; Blackburn, N. J. *Biochem. J.* **1984**, *221*, 545–548.

(14) McFadden, D. L.; McPhail, A. T.; Garner, C. D.; Mabbs, F. E. *J. Chem. Soc., Dalton Trans.* **1976**, 47–52.

(15) Ivarson, G. *Acta Chem. Scand.* **1973**, *27*, 3523–3530.

(16) Fransson, G.; Lundberg, B. K. S. *Acta Chem. Scand., Ser. A* **1974**, *28*, 578–588.

(17) (a) Gurman, S. J.; Binsted, N.; Ross, I. *J. Phys. C., Solid State Phys.* **1984**, *17*, 143–151. (b) Gurman, S. J.; Binsted, N.; Ross, I. *J. Phys. C, Solid State Phys.* **1986**, *19*, 1845–1861.

(18) (a) Lee, P. A.; Pendry, J. B. *Phys. Rev. B* **1975**, *11*, 2795–2811. (b) The angular dependence of the forward scattering and the contribution of multiple scattering to the total EXAFS are summarized in eq 2.1 and 3.1 of ref 18a. The forward scattering, which is energy dependent, peaks strongly at angles of $n\pi$, $n = 0, 1, 2, \ldots$, as shown in Figure 5 of reference 18a.

(19) Clementi, E.; Roetti, C. *Atomic Data and Nuclear Data Tables*; Academic: New York, 1974; Vol. *14*, No. 3–4.

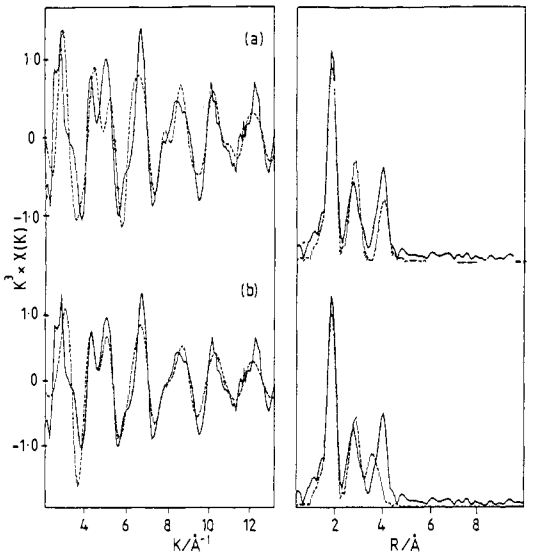

Figure 2. Single-scattering simulations of the EXAFS and Fourier transforms associated with the Cu K edge of tetrakis(imidazole)copper(II) nitrate: (a) calculations using distances determined by crystallography; (b) after refinement using the least-squares curve-fitting program EXCURVE. The k value used in the figure, and in subsequent figures, is defined as the experimental k value plus the E_0. Thus, k = 2.17 Å^{-1} (corresponding to E_0 = 17.69 eV, the value used in the calculations) represents the experimental absorption threshold.

tering amplitude was found to be larger than that calculated by single-scattering theory. The calculated phase shift was also found to be out of phase by approximately π with the observed fourth-shell phase. These effects were accounted for by recognizing that the first-shell copper atoms were directly in line between the central absorber atom and the fourth-shell atoms, producing a strong forward scattering of both outgoing and backscattered photoelectron wave. Similar enhancement of EXAFS amplitude has been observed and successfully quantified in the EXAFS of transition-metal carbonyls, where strong multiple-scattering interactions occur within the nearly collinear M–C–O groups.[17b] The magnitude of the forward scattering is highly directional and attenuates rapidly as the angle of scatter is decreased from 180°.[2a,18b,30] Thus, the strongest forward scattering occurs when the atoms involved are arranged collinearly, whereas for a scattering pathway of 90° the multiple scattering is negligible.[30]

In an imidazole ring (Figure 1), multiple scattering occurs due to strong forward scattering between the N1 shell and the N4/C3 and C2/C5 shells. The main multiple-scattering pathways are shown in Figure 1. For tetrakis(imidazole)copper(II) nitrate the scattering angles for pathways Cu–N1–N4/C3 and Cu–N1–C2/C5 are 163° and 125°, respectively. Since the individual single-scattering pathways contributing to the multiple-scattering pathways all lie in the same plane, these angles are sufficient to define the geometry of the multiple-scattering pathways in the calculations. The multiple-scattering contribution to the calculated EXAFS spectrum is obtained by summing the contributions from all the scattering pathways between the absorbing atom and the C2/C5 and C3/N4 atoms. The total EXAFS of the Cu atom therefore consists of direct backscattering contributions from the N1, C2/C5, and C3/N4 atoms (single scattering), plus the backscattering from the latter two shells via the first-shell nitrogen (multiple scattering).

Results

The crystal structure parameters for tetrakis(imidazole)copper(II) nitrate are given in Table I. Figure 2a shows the experimental EXAFS and Fourier transform compared with single-scattering theoretical simulations utilizing these parameters. (The Debye–Waller terms have been adjusted to fit the amplitude of the peaks in the Fourier transform.) Even though the agreement for the major peaks in the Fourier transform is good, the single-scattering theory is unable to reproduce the experimental EXAFS spectrum with these parameters. If the distances are now allowed to float within the least-squares refinement routine, an acceptable fit can be obtained (Figure 2b) with the first-shell nitrogens and second-shell carbons (C2/C5) close to their crystallographic values; however, the third-shell carbon and nitrogen atoms (C3/N4) refine some 0.3 Å shorter than their known distances (Table I), as has been found previously.[7] The origin of this foreshortening of outer-shell distances can be understood by filtering out their contribution to the EXAFS in the transform range $3.5 < R < 4.5$ Å. The resultant Fourier-filtered spectrum is shown in Figure 3a, together with the single-scattering EXAFS calculated from the crystallographically determined Cu–C3/N4 distances. A large phase difference, nearly equal to π is apparent between the two waves. It is in order to compensate for this phase difference that the third-shell distances are reduced by 0.3 Å in the least-squares refinement.

When the effects of multiple scattering are included in the calculations, a major improvement to the fit can be obtained (Figure 3b). The multiple-scattering contribution was calculated initially by using the crystal structure parameters given in Table I as described in the methods section. The final fit obtained by this procedure is shown in Figure 4a while the multiple-scattering contribution alone is shown in Figure 5. Figure 4 shows a clear improvement in the fit compared with that obtained by using single scattering only (Figure 2), and the fit parameters (Table I) are close to those of the crystal structure. The overall shape of the near edge or XANES region of the spectrum is also well reproduced, suggesting that the dominant multiple-scattering contri-

Table I. Parameters Used To Simulate the Cu K-Edge EXAFS Spectra of Tetrakis(imidazole)copper(II) Nitrate, Tetrakis(imidazole)copper(II) Perchlorate, Aquatris(imidazole)copper(II) Sulfate, and Freeze-Dried Cu/Zn Superoxide Dismutase[a]

		EXAFS			
	crystal structure	single scattering		multiple scattering	
shell	R_{av}/Å	R/Å	$2\sigma^2$/Å^2	R/Å	$2\sigma^2$/Å^2
	Tetrakis(imidazole)copper(II) Nitrate[14]				
4 N	2.00	2.00	0.005	2.00	0.005
4 C	2.98	2.92	0.010	2.92	0.007
4 C	3.04	3.02	0.010	3.02	0.007
4 C	4.14	3.78	0.010	4.15	0.010
4 C	4.18	3.87	0.010	4.22	0.010
	Tetrakis(imidazole)copper(II) Perchlorate[15]				
4 N	2.00	2.00	0.005	2.00	0.005
4 C	2.96	2.92	0.011	2.92	0.010
4 C	3.04	3.02	0.010	3.02	0.010
4 C	4.12	3.80	0.010	4.11	0.010
4 C	4.18	3.87	0.010	4.23	0.010
	Aquatris(imidazole)copper(II) Sulfate[16]				
3 N	1.99			1.99	0.006
1 O	2.01			1.96[b]	0.005
3 C	2.97			2.92	0.010
3 C	3.04			3.03	0.010
3 C	4.13			4.15	0.011
3 C	4.17			4.21	0.013
	Freeze-Dried Cu/Zn Superoxide Dismutase[7a]				
4 N		1.99	0.006	1.99	0.006
4 C		2.86	0.010	2.88	0.007
4 C		3.01	0.010	3.00	0.007
4 C		3.87	0.010	4.05	0.012
4 C		3.84	0.010	4.23	0.012

[a] The error associated with the bond lengths given in the table is ±0.02 Å for first-shell distances and ±0.05 Å for outer-shell distances. The Debye–Waller term ($2\sigma^2$) represents the root-mean-square relative displacement along the direction of the absorber–scatterer vector. [b] This distance is expected to have a higher error associated with it (±0.05 Å) because it is determined by least-squares minimization of a single oxygen atom within a shell of three equidistant nitrogen atoms. No real significance should be attached to any difference loss than ca. 0.10 Å between first-shell oxygen and nitrogen atoms.

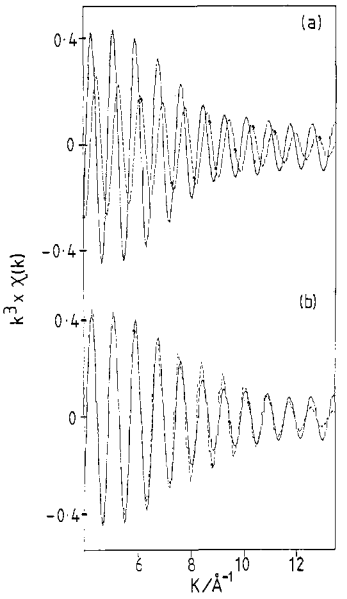

Figure 3. Simulation of the backtransformed third-shell EXAFS contribution (R = 3.5–4.5 Å^{-1}) of tetrakis(imidazole)copper(II) nitrate using crystallographic distances: (a) the phase problem which results from the use of single-scattering theory alone; (b) the fit to the third-shell obtained when multiple scattering is included. The backtransformation window was Gaussian.

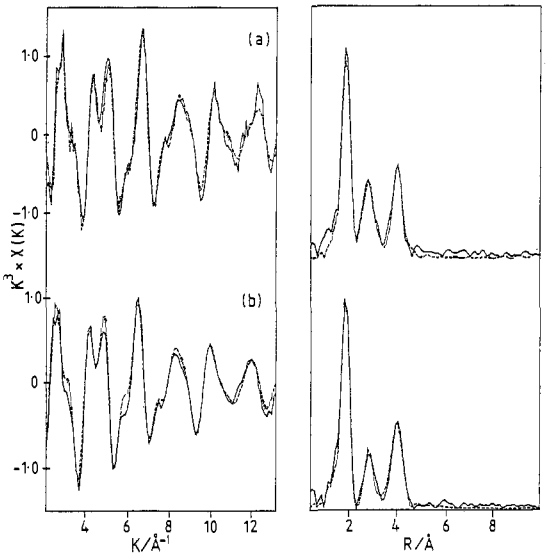

Figure 4. EXAFS simulations of the Cu K edge EXAFS and Fourier transform of copper–imidazole complexes including the multiple-scattering contributions: (a) tetrakis(imidazole)copper(II) nitrate; (b) tetrakis(imidazole)copper(II) perchlorate.

bution to the XANES is due to intra- rather than interligand scattering processes within the imidazole rings.

This analysis was repeated for tetrakis(imidazole)copper(II) perchlorate. A strong multiple-scattering contribution was again required to reproduce all the features of the EXAFS. The best simulation obtained is shown in Figure 4b, with the fit parameters given in Table I. They compare favorably with the crystallographic data.

Figure 6 shows the effect of introducing multiple scattering in the analysis of the EXAFS of a protein system, in this case the Cu K edge of lyophilized superoxide dismutase. Figure 6a shows the single-scattering simulation, which gives distances of 3.87 and 3.91 Å for the outer-shell atoms. In the multiple-scattering fit these distances refine to 4.05 and 4.23 Å, respectively.

The above results indicate that the inclusion of the multiple-scattering contribution leads to entirely satisfactory simulation of the experimental data for complexes involving imidazole groups

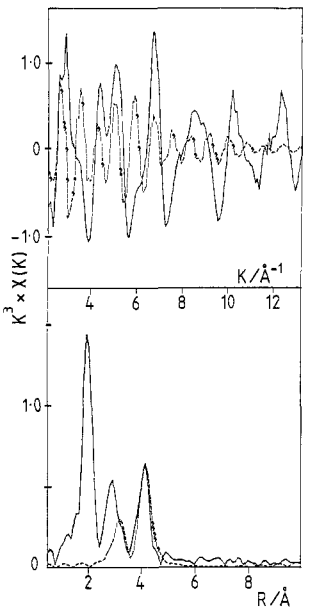

Figure 5. Comparison of the experimental spectrum for tetrakis(imidazole)copper(II) nitrate with the multiple-scattering contribution calculated for the four imidazole rings.

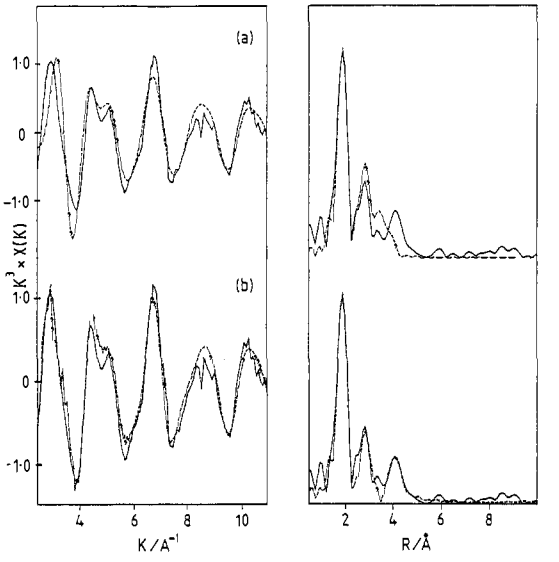

Figure 6. EXAFS simulations for the Cu K edge of freeze-dried bovine erythrocyite Cu/Zn superoxide dismutase: (a) using single scattering only; (b) including the multiple-scattering contribution.

as the only coordinated ligand. Many metalloproteins are known or believed to contain mixed coordination involving histidine together with other ligands such as water or hydroxyl (amine oxidase,[12b,c] oxyhemocyanin[20]), carboxylate from glutamate or aspartate (zinc site of superoxide dismutase,[11] Mn superoxide dismutase,[21] Fe in hemerythrin[22]), tyrosine (Fe in transferrin[23]), cysteine, and methionine (Cu in plastocyanin and azurin[24]) to

(20) (a) Himmelwright, R. S.; Eickman, N. C.; Solomon, E. I. *J. Am. Chem. Soc.* **1979**, *101*, 1576–1586. (b) Himmelwright, R. S.; Eickman, N. C.; LuBien, C. D.; Solomon, E. I. *J. Am. Chem. Soc.* **1980**, *102*, 5378–5388. (c) Gatkema, W. P. J.; Volbeda, A.; Hol, W. G. J. *J. Mol. Biol.* **1985**, *187*, 255–275.

(21) Stallings, W. C.; Pattridge, A. K.; Strong, R. K.; Ludwig, M. L. *J. Biol. Chem.* **1985**, *260*, 16424–16432.

(22) (a) Stenkamp, R. E.; Sieker, L. C.; Jensen, L. H. *J. Am. Chem. Soc.* **1984**, *106*, 618–622. (b) Stenkamp, R. E.; Sieker, L. C.; Jensen, L. H.; McCallum, J. D.; Sanders-Loehr, J. *Proc. Natl. Acad. Sci. U.S.A.* **1985**, *82*, 713–716.

(23) Garrett, R. C.; Evans, R. W.; Hasnain, S. S.; Lindley, P. F. *Biochem. J.* **1986**, *233*, 479–484.

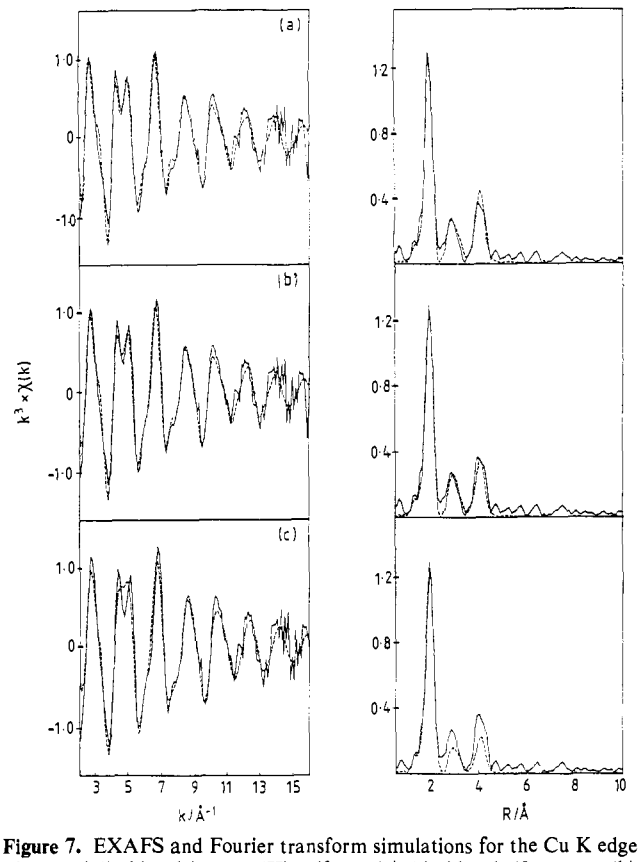

Figure 7. EXAFS and Fourier transform simulations for the Cu K edge of aquatris(imidazole)copper(II) sulfate: (a) 4 imidazole/0 oxygen; (b) 3 imidazole/1 oxygen; (c) 2 imidazole/2 oxygen. The distances and Debye–Waller terms were as given for the 3/1 fit in Table I.

name but a few examples. It is therefore of interest to determine whether the inclusion of multiple scattering in the simulations of EXAFS data will enable the determination of the number of coordinated imidazoles in such mixed-ligand systems.

To address this problem, we have compared the experimental EXAFS of the complex aquatris(imidazole)copper(II) sulfate, $[Cu(imid)_3H_2O]SO_4$, with simulations based on (a) four imidazoles, (b) three imidazoles and one O atom, and (c) two imidazoles and two O atoms. The results are shown in Figure 7a–c, respectively. The simulations all employ four first-shell scatterers and thus the quality of fit to the EXAFS at high k ($8 < k < 16$ Å^{-1}) and to the first peak in the Fourier transform is the same in each case. The low-energy ($2 < k < 8$ Å^{-1}) region of the EXAFS is expected to be most sensitive to the number of imidazole groups, and indeed a poor fit to this region is obtained for the two imidazole/two O (2/2) combination. However, the fits obtained for three imidazole/one O (3/1) and four imidazole/no O (4/0) combinations are visually and quantitatively comparable (least-squares differences (k^3 weighted) = 2.89 and 3.02, respectively). Examination of the imidazole outer-shell peaks in the Fourier transforms indicates that the amplitudes do indeed increase linearly as the number of imidazole groups is increased from two to four (peak amplitude = 0.23, 0.35, and 0.45, respectively), with the best fit corresponding to the 3/1 combination.

The following points emerge from the above analysis. (i) The 2/2 combination can be distinguished from 3/1 and 4/0. (ii) Provided the data are of high quality, it may be possible to distinguish between 3/1 and 4/0 on the basis of Fourier transform outer-shell amplitudes. (iii) Great care should be exercised in making distinctions between 3/1 and 4/0 on the basis of EXAFS simulations alone or when the quality and/or range of the data is limited since in such cases the amplitudes of Fourier transform peaks can be distorted significantly. The parameters used in the 3/1 fit of Figure 7b are given in Table I.

Discussion

The work presented here clearly demonstrates the importance of multiple scattering in the EXAFS of systems containing imidazole ligands. Strong multiple-scattering contributions are present in the EXAFS over an extended range above the absorption edge and these contributions are necessary to fix the third-shell atoms of imidazole groups at their correct positions. Furthermore, by including multiple scattering in the EXAFS analysis, it is possible to extend the low-energy fitting range to include the XANES region of the spectrum below $k = 3$, the general shape of this part of the spectrum being well reproduced. In favorable circumstances, the multiple-scattering approach can provide the basis for determining the number of histidine ligands in a mixed-ligand complex and can clearly distinguish between two and four coordinated imidazole groups, although distinction between three and four histidines is probably unrealistic for a site of unknown structure.

The inadequacies of single-scattering theory to account for outer-shell EXAFS of imidazole systems have been noted by other workers.[5,6,9] Co and Hodgson[4a] have described a group-fitting procedure for imidazole ligands which exploits the fact that the internal planar geometry of the imidazole group is always preserved, such that the coordinates of all the atoms of the ring should be determined by the metal to first-shell nitrogen distance. Their procedure overcame the differences in overall backscattering phase produced by the multiple-scattering processes (Figure 3) by artificially adjusting the phase shifts for each individual shell of atoms of chosen crystallographically characterized complexes, within a single-scattering approximation, and it was assumed that the modified phase shifts could be transferred to unknown systems. Their procedure allowed the EXAFS contributions of all the atoms of the imidazole rings to be correctly simulated, and the method was successfully applied to selected copper–imidazole and copper–histidine systems, including oxy-[4c] and deoxyhemocyanin.[4b] However, because of the strong angular dependence of the multiple scattering,[30] the resultant backscattering phase of the outer shells is expected to depend on ring orientation and will not be transferrable from model to protein unless the ring orientation of the model is preserved in the protein system. Existing evidence derived from detailed analysis of the EXAFS of coordinated histidines in Cu/Zn superoxide dismutase and its derivatives[7,25] suggests that this condition is not satisfied, since the imidazole groups are substantially tilted about the normal to the copper–nitrogen bond, with the degree of tilt dependent on the identity of the derivative,[26] and a similar situation is found in some copper–imidazole complexes where the proton attached to N4 of the ring forms a hydrogen bond to the counterion in the crystal.[27] Thus, while group fitting for imidazole is clearly advantageous because it decreases the number of parameters which have to be refined simultaneously,[28] such procedures can lead to an inadequate representation of the structure unless they are based on a multiple-scattering approach, rather than a single-scattering approach.

In conclusion we note that, since the methods described herein lead to an exact simulation of the experimental EXAFS for

(24) (a) Guss, J. M.; Freeman, H. C. *J. Mol. Biol.* **1983**, *169*, 521–563. (b) Norris, G. E.; Anderson, B. F.; Baker, E. N. *J. Am. Chem. Soc.* **1986**, *108*, 2784–2785.

(25) (a) Blackburn, N. J.; Hasnain, S. S. In *Biological and Inorganic Copper Chemistry*; Karlin, K. D., Zubieta, J., Eds.; Adenine: Guilderland, NY, 1986; Vol. II, pp 33–42. (b) Blackburn, N. J.; Strange, R. W.; McFadden, L.; Hasnain, S. S., submitted to *J. Am. Chem. Soc.*

(26) The asymmetry of imidazole ring coordination is inferred from (i) the observed differences of ca. 0.1–0.3 Å in (a) the average Cu–C2 and Cu–C5 distances and (b) the average Cu–C3 and Cu–N4 distances and (ii) different scattering angles for the Cu–N1–C2, Cu–N1–C5 and Cu–N1–C3, Cu–N1–N4 pathways.

(27) McFadden, D. L.; McPhail, A. T.; Garner, C. D.; Mabbs, F. E. *J. Chem. Soc., Dalton Trans.* **1975**, 263–268.

(28) The multiple-scattering approach locates all the atoms of the imidazole rings at their crystallographic positions and thus allows the imidazole ring to be treated as a unit. The radial distribution of imidazole ring atoms about Cu can therefore be described by the polar coordinates R, α, and β, where R is the metal–N1 distance and α and β are the angles between the Cu–N1 vector and (i) the ring plane and (ii) the vector bisecting the C2–N1–C5 angle (see Figure 1).

complexes of well-defined geometry, an alternative method for introducing stereochemical information into the refinement of an unknown system such as a metalloprotein is to treat the stereochemical conditions of fixed imidazole geometry as additional observations. This approach has been used in the least-squares refinement of Hendrickson and Konnert[29] for the crystallographic determination of protein structure, where a similar problem of underdeterminancy exists; i.e., the ratio of the number of observations to parameters is typically not more than two. We believe that such an approach combined with the multiple-scattering formalism will allow a more detailed and less ambiguous treatment, as well as offer the potential for extracting information relating to the degree of asymmetry of histidine coordination in metalloproteins.

Acknowledgment. We thank the Daresbury Laboratory for use of facilities. The work was carried out under a S.E.R.C. grant to N.J.B., P.F.K., and S.S.H. S.S.H. thanks Professor Charles E. Bugg (Director, Centre for Macromolecular Crystallography, University of Alabama at Birmingham) for his hospitality during a sabbatical stay.

(29) Hendrickson, W. A.; Konnert, J. H. *Proc. Madras Symp. Biomol. Struct. Conform. Function Evol.* **1981**, 43-57.
(30) Boland, J. J.; Crane, S. E.; Baldeschwieler, J. D. *J. Chem. Phys.* **1982**, *77*, 142-153.

Anion Binding to Bovine Erythrocyte Superoxide Dismutase Studied by X-ray Absorption Spectroscopy. A Detailed Structural Analysis of the Native Enzyme and the Azido and Cyano Derivatives Using a Multiple-Scattering Approach

Ninian J. Blackburn,*[1a] Richard W. Strange,[1a] Loretta M. McFadden,[1a] and S. Samar Hasnain[1b]

Contribution from the Department of Chemistry, University of Manchester Institute of Science and Technology, Manchester, M60 1QD, United Kingdom, and S.E.R.C. Daresbury Laboratory, Warrington, Cheshire, WA4 4AD, United Kingdom. *Received January 30, 1987*

Abstract: X-ray absorption spectra are reported for the native, azide-bound, and cyanide-bound forms of bovine erythrocyte superoxide dismutase (SOD). Absorption edge data suggest a similar geometric structure for the native enzyme and the azido derivative, but a different coordination structure for the cyano derivative. Analysis of the EXAFS, using a recently developed multiple-scattering method for treating systems containing metal-histidine coordination, has allowed accurate simulation of the raw unfiltered EXAFS data over the range k = 3-13 Å^{-1}. The analysis has provided structural details of the coordinated imidazole rings in addition to structural parameters for the coordinated anions. Thus azide is coordinated in an equatorial position of a square-pyramidal site, with Cu-N(azide) = 1.99 Å and a Cu-N-N angle of less than ca. 135°. The cyanide group is also coordinated in an equatorial position, with Cu-C = 1.97 Å and a Cu-C-N angle of 180°. The multiple-scattering analysis of the linear Cu-C-N group has allowed determination of the C-N distance of the cyano group as 1.18 Å. Unlike azido-SOD, which retains an axial imidazole group at 2.27 Å, the cyano derivative appears to be 4-coordinate, with no evidence for an additional coordinated histidine. Detailed analysis of the outer-shell contributions from the coordinated histidine groups indicates that the imidazole rings are asymmetrically coordinated, with the degree of asymmetry depending on the identity of the derivative. It is suggested that the latter effect results from alteration in N_δ-H-bonding interactions of the coordinated imidazoles with the polypeptide chain.

Interest in the Cu/Zn superoxide dismutase (SOD) stems both from its well-defined coordination chemistry and from the growing importance of its pharmaceutical properties.[2] The enzyme is invoked increasingly as a model for non-blue copper proteins[3] since it exhibits many of the chemical and spectroscopic properties of this class of enzymes, including the ability to bind anions,[2,4,5] but remains the only member for which a high-resolution crystal structure is available.[6] The dismutation of superoxide (eq 1) is

$$2HO_2^{\bullet -} = O_2 + H_2O_2 \quad (1)$$

catalyzed by the copper atom, which is coordinated to four histidine residues in the oxidized form, one histidine forming a bridge to the neighboring zinc atom. The stereochemistry at both copper and zinc approximates to a flattened tetrahedron. An essential arginine residue (Arg-141)[7] is located in the active-site pocket

(1) (a) Department of Chemistry, University of Manchester Institute of Science and Technology, U.K. (b) S.E.R.C. Daresbury Laboratory, Warrington, Cheshire, U.K.
(2) (a) Valentine, J. S.; Pantoliano, M. W. In *Copper Proteins*; Spiro, T. G., Ed.; Wiley: New York, 1981; pp 291-358. (b) Fee, J. A. In *Metal Ions in Biological Systems*; Sigel, H., Ed.; Marcel Dekker: New York, 1981; Vol. 13, pp 259-298. (c) Fielden, G. M.; Rotilio, G.; In *Copper Proteins and Copper Enzymes*; Lontie, R., Ed.; CRC Press: Boca Raton, FL, 1984; Vol. 2, pp 27-61. (d) Cass, A. E. In *Metalloproteins, Part I: Metal Proteins with Redox Roles*; Harrison, P. M., Ed.; Macmillan: London, 1985; pp 121-156. (e) Steinman, H. M. In *Superoxide Dismutase*; Oberly, L., Ed.; CRC Press: Boca Raton, FL, 1982; Vol. I, pp 11-68. (f) Forty-eight papers on the pharmacological and clinical aspects of superoxide and superoxide dismutase have been published in *Superoxide and Superoxide Dismutase in Chemistry, Biology and Medicine*, Proceedings of the 4th International Conference on Superoxide and Superoxide Dismutase, Rome, 1985; Rotilio, G., Ed.; Elsevier: Amsterdam, 1986; pp 493-681.
(3) Malkin, R.; Malmstrom, B. G. *Adv. Enzymol.* **1970**, *33*, 177-244.
(4) (a) Fee, J. A.; Gaber, B. P. *J. Biol. Chem.* **1972**, *247*, 60-65. (b) Bertini, I.; Borghi, E.; Luchinat, C.; Scozzafava, A. *J. Am. Chem. Soc.* **1981**, *103*, 7779-7783. (c) Dooley, D. M.; McGuirl, M. A. *Inorg. Chem.* **1986**, *25*, 1261-1264.
(5) Blackburn, N. J.; Collison, D.; Sutton, J.; Mabbs, F. E. *Biochem. J.* **1984**, *220*, 447-454. (b) Barker, R.; Boden, N.; Cayley, G.; Charlton, S. C.; Henson, R.; Holmes, M. C.; Kelly, I. D.; Knowles, P. F. *Biochem. J.* **1979**, *177*, 289-302. (c) Dooley, D. M.; Cote, C. E. *Inorg. Chem.* **1985**, *24*, 3996-4000. (d) Giordano, R. S.; Bereman, R. D.; Kosman, D. J.; Ettinger, M. J. *J. Am. Chem. Soc.* **1974**, *96*, 1023-1026.
(6) (a) Tainer, J. A.; Getzoff, E. D.; Beem, K. M.; Richardson, J. S.; Richardson, D. C. *J. Mol. Biol.* **1982**, *160*, 181-217. (b) Tainer, J. A.; Getzoff, E. D.; Richardson, J. S.; Richardson, D. C. *Nature (London)* **1983**, *306*, 284-287.

0002-7863/87/1509-7162$01.50/0